Sensors and Actuators B 159 (2011) 60–65

Contents lists available at ScienceDirect

Sensors and Actuators B: Chemical

journal homepage: www.elsevier.com/locate/snb

# On-chip Fabry–Pérot interferometric sensors for micro-gas chromatography detection

Karthik Reddy[a,b], Yunbo Guo[a], Jing Liu[a,c], Wonsuk Lee[a,b], Maung Kyaw Khaing Oo[a], Xudong Fan[a,c,*]

[a] Department of Biomedical Engineering, University of Michigan, 1101 Beal Avenue, Ann Arbor, MI 48109, United States
[b] Department of Electrical Engineering and Computer Science, University of Michigan, 1301 Beal Avenue, Ann Arbor, MI 48109, United States
[c] Engineering Research Center for Wireless Integrated Microsystems, University of Michigan, 1301 Beal Avenue, Ann Arbor, MI 48109, United States

ARTICLE INFO

*Article history:*
Received 13 April 2011
Received in revised form 31 May 2011
Accepted 9 June 2011
Available online 15 June 2011

*Keywords:*
Vapor sensing
Optical vapor sensor
Fabry–Pérot cavity
Micro-gas chromatography
Volatile organic compounds

ABSTRACT

We fabricated and characterized on-chip Fabry–Pérot (FP) vapor sensors for the development of on-column micro-gas chromatography (μGC) detectors. The FP sensors were made by coating a thin layer of polymer on a silicon wafer. The air–polymer and polymer–silicon interfaces form an FP cavity, whose resonance wavelengths change in response to the vapor absorption/desorption, thus allowing for rapid detection and quantification of vapors. For proof-of-concept, two polymers (PDMS and SU-8) were used independently and placed in an array in a microfluidic channel, and showed different sensitivities for different vapors. A sub-nano-gram detection limit and sub-second response time were achieved, representing orders of magnitude improvement over those previously reported. This on-chip design will enable the unprecedented integration of optical vapor sensors with μGC systems.



## 1. Introduction

Detection of volatile organic compounds (VOCs) is of importance for many applications in homeland security, environmental and industrial monitoring, healthcare, and battlefields [1,2]. Traditional gas chromatography systems show excellent detection specificity and sensitivity; however, they are bulky and have high power consumption. Applications of on-site, rapid, and real time VOC analysis require innovative portable micro-gas chromatography (μGC) systems, which have been under intense study in the past couple of decades [3–5]. In addition to the development of miniaturized on-chip micro-fabricated columns, micro-pumps, and micro-heaters [6–10], significant effort has been focused on developing micro-vapor detectors that need to be sensitive, fast in response, small in size, and easily integrated with other μGC components.

Optical based sensors are one of the most promising gas sensing technologies. As compared to their electrical based counterparts, such as chemiresistor sensor arrays [11], carbon black sensors [12], and carbon nanotube sensors [13], they are immune to electromagnetic interference and do not generate any electric field that could be undesirable in sensitive environments. Through years of research, various configurations of optical gas sensors have been explored, including surface plasmon resonance (SPR) sensors [14,15], ring resonator sensors [16–19], fiber Bragg grating sensors [20–22], long period fiber grating sensors [23–25], photonic crystal fiber sensors [26], and Fabry–Pérot (FP) type sensors [27–32]. While sensitive, the SPR, fiber grating, and photonic crystal based sensors are difficult to integrate with micro-columns due to their relatively bulky configurations. The capillary based thin-walled ring resonator is the first optical gas sensor that can be fully integrated with μGC, as the capillary serves as both GC column and on-column gas detector [17,18]. However, mass-production of those ring resonators with high reproducibility and mechanical strength has yet to be worked out.

In contrast, FP-based sensors are robust, and display the potential for mass production and simple integration with current μGC technology. For an FP sensor, the gas sensing polymer forms part of the FP cavity. When exposed to VOCs, the polymer thickness or refractive index (RI) changes, thus resulting in the sensing transduction signal. Recently, Liu et al., fabricated fiber tip based FP sensors using the dip-coating method [30,31]. While these sensors can be integrated with μGC systems and are capable of rapid on-column detection of separated analytes with excellent sensitivity [30], they suffer from lack of control and variability in the deposition of gas sensing polymer layers. Fabrication of the FP gas sensor on a flat glass substrate has also been explored [27,28,32], in which the gas sensitive polymer can easily be spin-coated on the glass with better thickness control. However, their setups are

* Corresponding author at: Department of Biomedical Engineering, University of Michigan, 1101 Beal Avenue, Ann Arbor, MI 48109, United States.
Tel.: +1 734 763 1273; fax: +1 734 647 4834.
*E-mail address:* xsfan@umich.edu (X. Fan).

0925-4005/$ – see front matter © 2011 Elsevier B.V. All rights reserved.
doi:10.1016/j.snb.2011.06.041

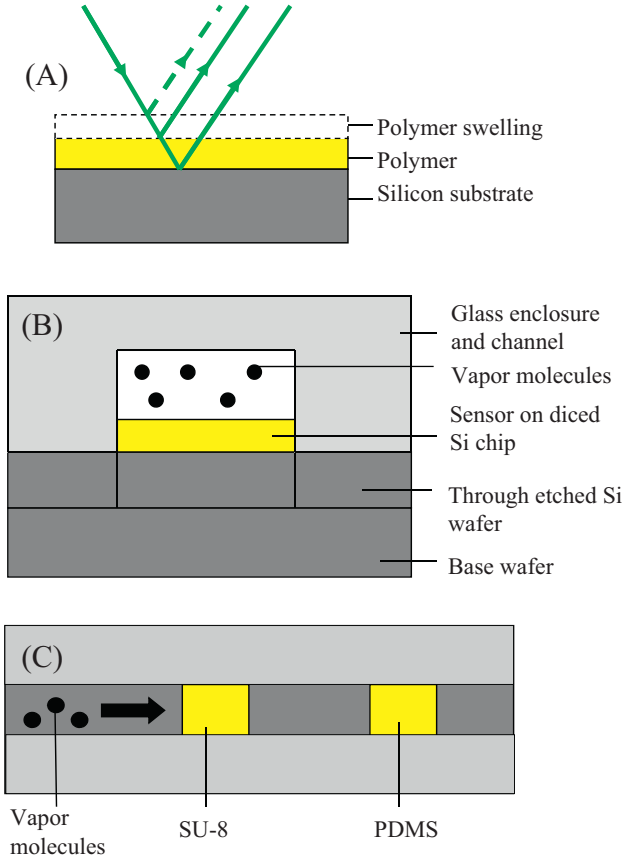


**Fig. 1.** (A) Schematic of the Fabry–Pérot (FP) sensor. The polymer spin-coated on a prime grade silicon wafer forms a smooth and controllable vapor sensing layer. The thickness and the RI change in the polymer caused by the absorption of analytes result in a change in the reflected interference signal. (B) Cross-sectional view of the FP sensor configuration inside a microfluidic channel. (C) Top view of the FP sensors coated with different polymer and placed in series. In current experiments, the microfluidic channel was 1 mm deep and 250 μm wide. In the sensor array configuration in (C), two FP sensors were separated by 3 mm.

complicated and slow in response, making it difficult to integrate and perform real-time on-column gas measurement with μGC systems. In addition, due to the very small RI difference between the polymer (~1.4) and the glass substrate (~1.5), the sensitivity of those sensors may be compromised.

Here we developed an FP gas sensor fabricated on a silicon wafer, as shown in Fig. 1, which can be integrated with a μGC system for rapid and sensitive detection of VOCs. This FP sensor design provides a number of distinct advantages compared to previous ones. First, due to the large RI difference between the polymer ($n$ = 1.4–1.7) and silicon ($n$ = 3.4–4), a larger contrast in the interference signal and hence higher detection sensitivity can be achieved. Second, use of prime grade silicon wafers as the substrate instead of glass significantly minimizes substrate roughness, which leads to low noise during detection. Third, spin-coating instead of dip-coating, used in our work, increases polymer film uniformity and fabrication controllability. Fourth, our design enables sub-micron polymer film, which greatly increases the detection speed. Finally, the on-chip design allows for excellent integration with current μGC separation columns fabricated on a silicon wafer and makes it ideal for mass production. Multiple sensors coated with various polymers can be fabricated in an array to further enhance the gas sensing performance.

In this paper, we report the FP sensor fabrication and integration with a GC column. Characterization of the sensor under pulsed gas flow shows that our sensor is capable of detecting sub-nano-gram mass of vapor analytes with a response time faster than 1 s. The simultaneous response of the FP sensor array to different analytes is also presented.

## 2. Theory

An FP cavity creates an interference pattern due to reflection at the polymer–air and polymer–silicon interfaces (see Fig. 1(A)). The reflected light intensity, $I(\lambda)$, is governed by:

$$I(\lambda) = R_1 + R_2 + 2\sqrt{R_1 R_2}\ \cos(\phi) \quad (1)$$

where $I$ is intensity of light and $\lambda$ is wavelength. $R_1$ and $R_2$ are the reflection coefficients at the polymer–air and polymer–silicon interfaces, respectively. For the normal incident light, $R_1$ and $R_2$ are approximately 16% and 5%, respectively.

$$\phi = \frac{4\pi n t\ \cos(\theta)}{\lambda} \quad (2)$$

where $n$ and $t$ are the polymer RI and thickness, respectively. $\theta$ is the incident angle in polymer. Any change in polymer RI and thickness due to the interaction with the analyte vapor will cause the interference pattern to shift, which in turn causes a change in intensity of the measured signal for a given wavelength, thus generating quantitative and temporal information about the presence of the analyte. The contrast ratio of the interference pattern is one of the important characteristics to determine the FP sensor sensitivity. Using the silicon wafer, the contrast ratio at the normal (45°) is 0.86 (0.94), which compares very favorably with a similarly configured FP sensor built on a glass substrate, which has a contrast ratio of only 0.46 (0.33).

## 3. Materials and methods

### 3.1. Materials

All the analytes used in the experiments were purchased from Sigma (St. Louis, MO) and had purity greater than 97%. GC guard column (part no. 22335, inner diameter 250 μm) was purchased from Restek (Bellefonte, PA). Universal quick seal column connectors were purchased from Varian (Palo Alto, CA). Silicon wafers were purchased from University Wafer (South Boston, MA). Poly(dimethylsiloxane) (PDMS) was purchased from Fluka (St. Louis, MO) and SU-8 2000.5 was purchased from MicroChem Corp. (Newton, MA). Glass slides were purchased from VWR (Radnor, PA). UV-curable optical glue was purchased from Dymax (Torrington, CT). All materials were used as received.

### 3.2. Sensor preparation

The on-chip FP sensor was prepared by spin-coating a polymer layer on a silicon wafer. The silicon wafer was first diced into a 2.5 cm × 2.5 cm piece. It was then cleaned by immersion in sulfuric acid-dichromate solution overnight, followed by deionized water rinsing. Finally, it was placed under UV light for an hour to ensure removal of any residues.

During experiments we used two polymers, PDMS and SU-8 2000.5, for the FP sensors. PDMS has been extensively used in gas chromatography and SU-8 is a common photoresist used in microfabrication. Both of them can form thin and uniform layers when spin coated [33]. The PDMS was diluted with toluene (PDMS:toluene = 1:4), whereas SU-8 was used as it was. After spin coating, PDMS and SU-8 were soft baked at 120 °C and 95 °C, respectively, to remove solvents. The polymer thicknesses were 1.2 μm

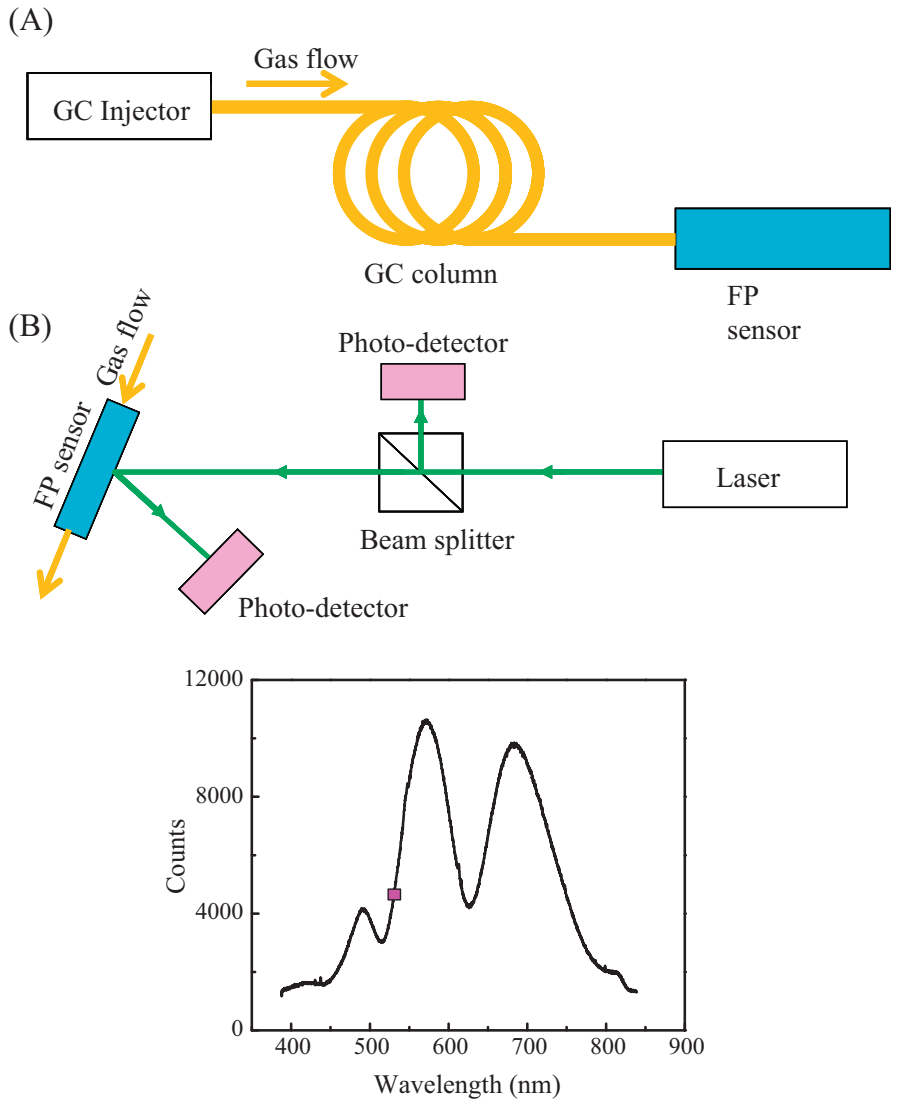


**Fig. 2.** (A) Schematic of the flow setup. The FP sensor was encased in a microfluidic channel shown in Fig. 1(B), and then connected to a GC injection port through a 5 m long GC guard column. (B) Schematic of the optical detection setup. A 532-nm laser was split into two beams, one for sensing, which measured the reflected intensity change induced by the VOCs inside the channel, and the other one for reference. The incident angle was adjusted to maximize the sensitivity. (C) Example of the interference spectrum from the light reflected from an FP sensor coated with 1.2 μm PDMS film. The incident angle was 10°. The square on the reflection curve indicates the spectral position of the 532-nm laser used in the experiment.

and 0.8 μm for PDMS and SU-8, respectively. To embed the FP sensor inside a microfluidic channel, an open-top channel was first formed by gluing glass slides together using UV-curable glue and subsequently bonded to the FP sensor wafer (see Fig. 1(B)). The microfluidic channel was 1 mm deep and 250 μm wide.

For the study of FP sensor array, a silicon wafer was diced into 8 mm × 8 mm pieces, which were spin-coated with the desired polymer according to the procedures described previously. To align the FP sensors inside the microfluidic channel, 8 mm × 8 mm through-holes were etched on another silicon wafer, of the same thickness as the FP sensor wafer, using MA-6 and STS Pegasus Deep Reactive Ion Etching tools for photolithography and etching, respectively. Then the FP sensors were inserted into the etched wafer and bonded into place (see Fig. 1(B) and (C)). The FP sensors installed in this manner ensured that the sensing surface (*i.e.*, the polymer layers) was nearly flush with the microfluidic channel surface so as not to disturb the gas flow. In the experiment, an array of two FP sensors coated with PDMS and SU-8 were used. They were separated by 3 mm inside the microfluidic channel.

### 3.3. Experimental setup

The experimental setup is illustrated in Fig. 2(A) and (B). Injection of analytes was carried out by the GC injector. The injected mass was calibrated with mass spectrometry. A 5 m long guard column was used to deliver the analytes to the FP sensor module. Helium was used as the carrier gas with a flow rate of 8 mL/min.

For optical detection, a 532-nm diode laser was split into two beams. One was reflected from the FP sensor and the other served as the reference. The intensity of both beams was recorded in real time by photo-detectors for post-analysis. The data acquisition rate was 90 kHz. A white light source aligned co-linearly with the laser was used in conjunction with a spectrometer (Ocean Optics HR-2000) to obtain the interference spectrum, an example of which is depicted in Fig. 2(C). This allowed us to optimize the incident angle, thus positioning the laser near the quadrature point of the FP sensor interference spectrum for the most sensitive measurement. For the array of sensors two sensing beams were used to interrogate the two sensors separately, which allowed us to tune the sensors independently to maximize the sensi-

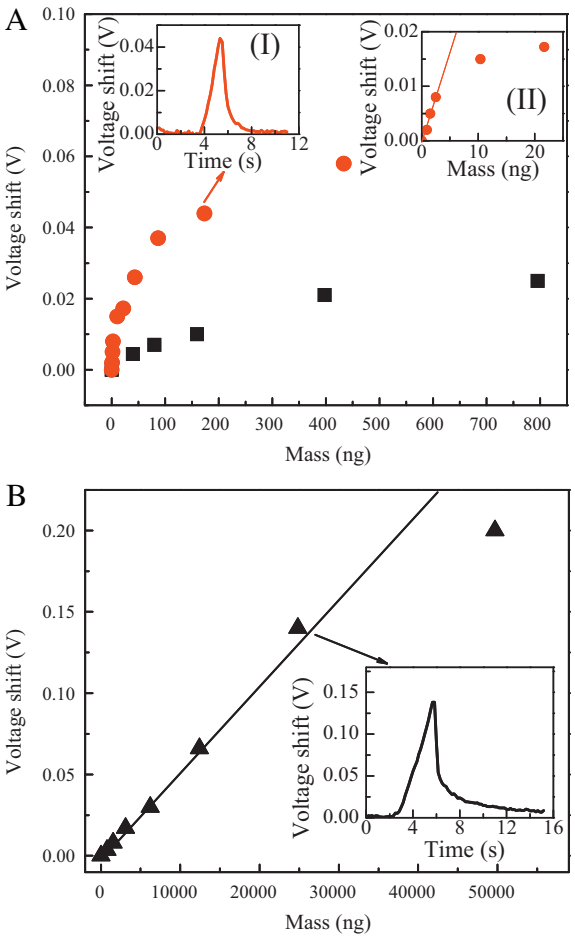


**Fig. 3.** (A) Response of PDMS FP sensor to toluene (circles) and acetone (squares) with various injected masses. *Inset I*: Temporal response of the PDMS FP sensor to the injection of 175 ng of toluene. *Inset II*: Magnified part shows PDMS sensor response to toluene with injected mass from 1 to 25 ng. The sensitivity of 2900 μV/ng is obtained through a linear fit shown by the solid line. (B) Response of SU-8 FP sensor to acetone at various injected masses. The sensitivity of 4 μV/ng is obtained through a linear fit shown by the solid line. Inset shows the temporal response of the SU-8 FP sensor to the injection of 23 μg of acetone.

tivity and response of each sensor. In all experiments, the GC column and the FP sensor modules were kept at room temperature.

## 4. Results and discussion

Inset I in Fig. 3(A) presents a typical temporal response of an FP sensor to the pulsed analyte. The signal rises quickly upon the arrival of the analyte and returns to baseline, indicating that the analyte is completely purged. The peak value of the response of the two FP sensors coated respectively with PDMS and SU-8 to different analytes is plotted in Fig. 3. The sensitivity depends on the interaction of the analyte with polymer, which in turn depends on the nature of the polymer as well as the analyte's polarity, molecular weight, functional groups and volatility. PDMS is a non-polar polymer and exhibits significantly different interactions with toluene, a non-polar analyte, and acetone, a polar analyte (see Fig. 3(A)). The response to toluene shows a near linear variation with mass below 20 ng, with sensitivity of about 2900 μV/ng (see Inset II) and then starts to saturate afterwards. Given the system noise of 600 μV, the above sensitivity results in a detection limit of 200 pg in mass. Based on the retention time (5 s) and the peak width (1.2 s) obtained from Inset I, as well as the inner diameter (250 μm) and length (5 m) of the GC column, the above mass detection limit corresponds to a detection limit of approximately 1.7 ppm in concentration at atmospheric pressure, which is about one to three orders of magnitude better than 30–1500 ppm reported for the FP sensor in Ref. [32] that used the same polymer. In contrast, the sensitivity for acetone is measured to be only 46 μV/ng, much lower than that for toluene. The corresponding detection limit is 13 ng in mass (or 202 ppm in concentration). While using the same analyte (acetone), the SU-8 sensor shows a similar linear variation with injected mass. The sensitivity of the SU-8 sensors is approximately 4 μV/ng which leads to a detection limit of about 150 ng in mass (or 2336 ppm in concentration).

Rapid detection is crucial in μGC development. Since the data acquisition rate can be over 100 kHz, the FP sensor response is mainly determined by the analyte diffusion processes in the polymer. Therefore, thin polymer films will absorb analytes faster and be purged of analytes faster than thicker films. Fig. 4(A)–(C) shows that the response time (*i.e.*, full width half maximum of the peak) of the PDMS FP sensor for toluene and acetone is 0.9 s and 0.5 s, respectively, two orders of magnitude shorter than those reported in Ref. [32], which is too slow to be used in a μGC system due to the much thicker polymer layer (8.2 μm).

Note that as the vapor peak width may get broadened after the vapor pulse travels along the 5 m long GC column, the intrinsic FP sensor response time may be obscured. To further characterize the sensing performance of the FP sensors, we also used a flame ionization detector (FID) in replacement of the FP sensor module to detect the analyte. FID measures the vapor pulse instantaneously and therefore provides the actual width of the vapor pulse traveling inside the GC column (see Fig. 4(D)). For toluene, the FP sensor is nearly 0.43 s broader than the vapor pulse inside the GC column. This additional delay is caused by the relatively slow diffusion process of toluene molecules into and out of PDMS because of their relatively strong interaction. In comparison, the response of the FP sensors to acetone (see Fig. 4(B) and (C)) is nearly the same as the vapor pulse width, owing to the weak interaction between acetone and the polymer. The difference in response time agrees well with the different detection sensitivities of the PDMS FP sensor for toluene and acetone, as discussed previously. Additionally, by comparing Inset I in Figs. 3(A) and 4(A) we observe significant broadening of the response time, which is more pronounced as the injected mass is increased, and can lead to a response time as large as 3–5 s with an injected mass of 1–2 μg. This broadening effect is due to the overloading of analyte in the polymer, as evidenced by the saturation behavior of the FP sensor at large injected mass in Fig. 3(A).

Implementation of a sensor array that has different response patterns for different vapor analytes can significantly improve the analyte identification capability of a μGC system [5]. The on-chip FP sensor developed here is well suited for such applications. In the proof-of-concept experiment, the two FP sensors coated respectively with PDMS and SU-8 were embedded within a microfluidic channel and separated by 3 mm (see Fig. 1(C)). Since the linear speed of the analyte inside the microfluidic channel is very high (usually a few meters per second), these two sensors detect an analyte traveling along the channel virtually simultaneously. Fig. 5 shows the response of the two FP sensors to various combinations of VOCs. Both FP sensors exhibit response proportional to the analyte mass. The results show that the rapid response of the sensors can be effectively used to detect analytes separated through the columns while also giving us important quantification information. Additionally different polymers have different sensitivities with different analytes which can be used as a method to differentiate analytes. This method can be quite useful when co-elution of analytes occurs.

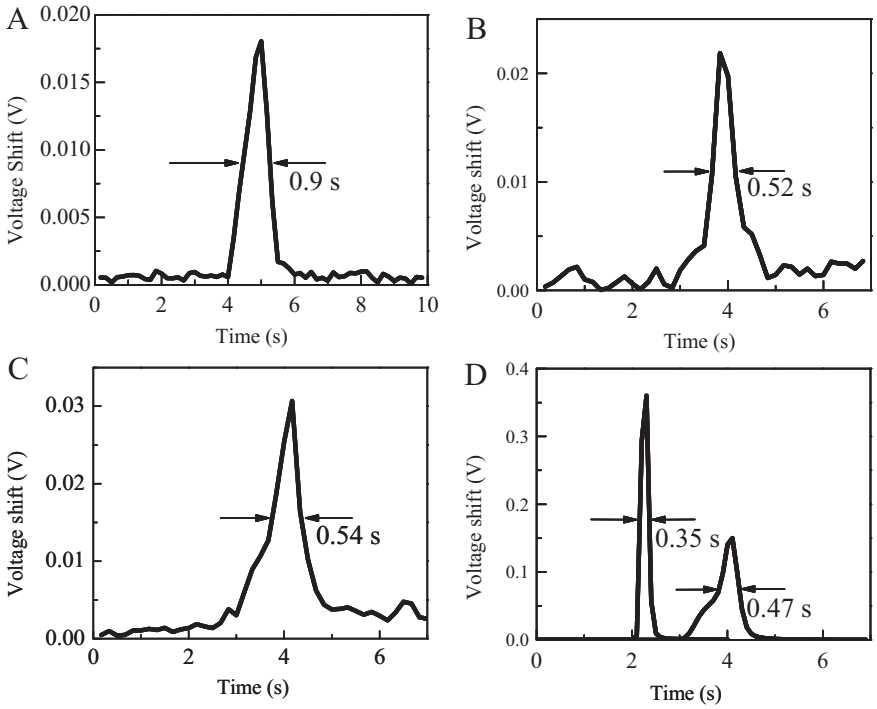


**Fig. 4.** Temporal response of PDMS FP sensor to (A) 20 ng of toluene and (B) 390 ng of acetone. (C) Temporal response of SU-8 sensor to 6 μg of acetone. (D) FID response to acetone and toluene. Peaks are horizontally shifted for clarity.

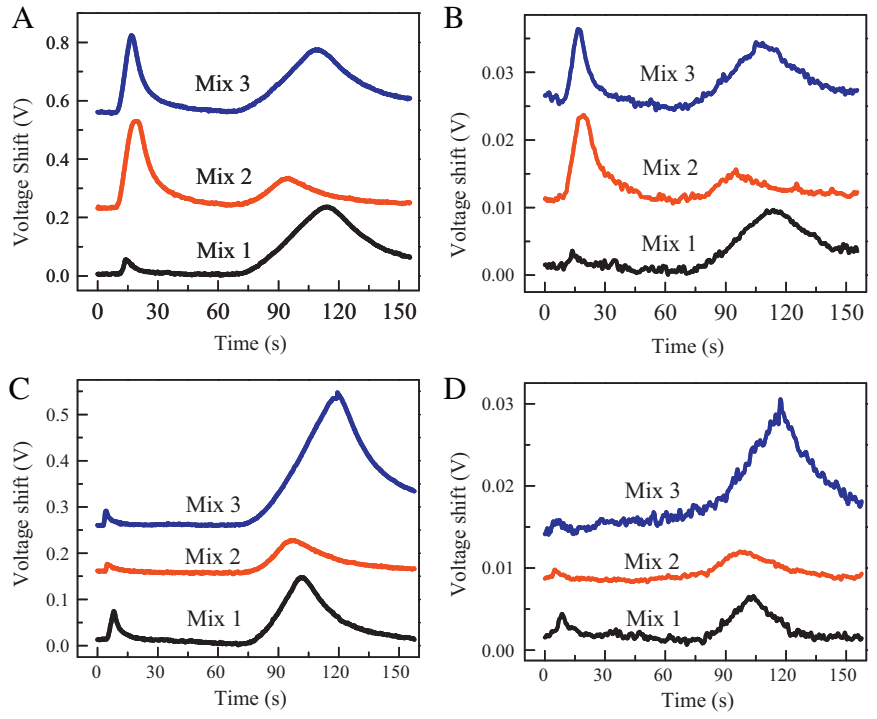


**Fig. 5.** (A) and (B) Real time response of the FP sensor array ((A): PDMS and (B): SU-8) to 3 different mixtures of octane and decane. Mix 1: 1.5/3.2 μg, Mix 2: 3.0/1.6 μg, and Mix 3: 3.0/3.2 μg for octane/decane, respectively. (C) and (D) Real time response of the FP sensor array. ((C): PDMS and (D): SU-8) to 3 different mixtures of acetone and decane. Mix 1: 1.6/2.4 μg, Mix 2: 0.8/1.6 μg, and Mix 3: 0.4/3.2 μg for acetone/decane, respectively.

## 5. Conclusion and future work

We have presented robust, simple, on-chip FP sensors that can potentially be integrated with a μGC system for rapid and sensitive VOC detection. A sub-nano-gram detection limit and sub-second detection time have been achieved, both of which are a few orders of magnitude better than those previously reported. To fully exploit the potential of this on-chip FP sensor, future work will be focused on the following aspects. First, a series of polymers will be explored to further enhance the detection sensitivity. Second, a sensor array consisting of more FP sensors (for example, 4 FP sensors) coated with different polymers will be inte-

grated within 1 mm, along a microfluidic channel to improve the detection specificity. Meanwhile, an optical imaging system will be implemented to accommodate the sensor array having larger number of FP sensors and to simultaneously monitor their response in real time. Finally, a complete FP sensor based μGC system comprised of micro-preconcentrators, micro-pumps, micro-valves, and micro-fabricated GC columns will be built to address the actual needs in environmental monitoring, homeland security, and healthcare.

## Acknowledgments

This work was supported by the National Science Foundation (IOS 0946735) and the Lurie Nanofabrication Facility at the University of Michigan, a member of the National Nanotechnology Infrastructure Network (NNIN) funded by the NSF.

## References

[1] E.J. Staples, S. Viswanathan, Ultrahigh-speed chromatography and virtual chemical sensors for detecting explosives and chemical warfare agents, IEEE Sens. J. 5 (2005) 622–631.
[2] F.L. Dorman, J.J. Whiting, J.W. Cochran, J. Gardea-Torresdey, Gas chromatography, Anal. Chem. 82 (2010) 4775–4785.
[3] E.S. Kolesar Jr., R.R. Reston, Review and summary of a silicon micromachined gas chromatography system, IEEE Trans. Comp., Pack., Manuf. Tech., Part B: Adv. Pack. 21 (1998) 324–328.
[4] E.B. Overton, K.R. Carney, N. Roques, H.P. Dharmasena, Fast GC instrumentation and analysis for field applications, Field Anal. Chem. Technol. 5 (2001) 97–105.
[5] C.-J. Lu, J. Whiting, R.D. Sacks, E.T. Zellers, Portable gas chromatograph with tunable retention and sensor array detection for determination of complex vapor mixtures, Anal. Chem. 75 (2003) 1400–1409.
[6] S.C. Terry, J.H. Jerman, J.B. Angell, A gas chromatographic air analyzer fabricated on a silicon wafer, IEEE Trans. Electron. Devices 26 (1979) 1880–1886.
[7] N. Hong-seok, P.J. Hesketh, G.C. Frye-Mason, Parylene gas chromatographic column for rapid thermal cycling, J. Microelectromech. Syst. 11 (2002) 718–725.
[8] M. Agah, J.A. Potkay, G. Lambertus, R. Sacks, K.D. Wise, High-performance temperature-programmed microfabricated gas chromatography columns, J. Microelectromech. Syst. 14 (2005) 1039–1050.
[9] G.R. Lambertus, C.S. Fix, S.M. Reidy, R.A. Miller, D. Wheeler, E. Nazarov, R. Sacks, Silicon microfabricated column with microfabricated differential mobility spectrometer for GC analysis of volatile organic compounds, Anal. Chem. 77 (2005) 7563–7571.
[10] S. Reidy, D. George, M. Agah, R. Sacks, Temperature-programmed GC using silicon microfabricated columns with integrated heaters and temperature sensors, Anal. Chem. 79 (2007) 2911–2917.
[11] Q.-Y. Cai, E.T. Zellers, Dual-chemiresistor GC detector employing monolayer-protected metal nanocluster interfaces, Anal. Chem. 74 (2002) 3533–3539.
[12] F. Zee, J. Judy, MEMS chemical gas sensor, in: P Thirteenth Biennial Univ./Gov./Ind. Microelectronics Symp., 1999, pp. 150–152.
[13] M. Stadermann, A.D. McBrady, B. Dick, V.R. Reid, A. Noy, R.E. Synovec, O. Bakajin, Ultrafast gas chromatography on single-wall carbon nanotube stationary phases in microfabricated channels, Anal. Chem. 78 (2006) 5639–5644.
[14] B. Liedberg, C. Nylander, I. Lunström, Surface plasmon resonance for gas detection and biosensing, Sens. Actuators 4 (1983) 299–304.
[15] C. de Julián Fernández, M.G. Manera, G. Pellegrini, M. Bersani, G. Mattei, R. Rella, L. Vasanelli, P. Mazzoldi, Surface plasmon resonance optical gas sensing of nanostructured ZnO films, Sens. Actuators B: Chem. 130 (2008) 531–537.
[16] A. Ksendzov, M.L. Homer, A.M. Manfreda, Integrated optics ring-resonator chemical sensor with polymer transduction layer, Electron. Lett. 40 (2004) 63–65.
[17] S.I. Shopova, I.M. White, Y. Sun, H. Zhu, X. Fan, G. Frye-Mason, A. Thompson, S.-J. Ja, On-column micro gas chromatography detection with capillary-based optical ring resonators, Anal. Chem. 80 (2008) 2232–2238.
[18] Y. Sun, J. Liu, D.J. Howard, G. Frye-Mason, A.K. Thompson, S.-J. Ja, X. Fan, Rapid tandem-column micro-gas chromatography based on optofluidic ring resonators with multi-point on-column detection, Analyst 135 (2010) 165–171.
[19] N.A. Yebo, P. Lommens, Z. Hens, R. Baets, An integrated optic ethanol vapor sensor based on a silicon-on-insulator microring resonator coated with a porous ZnO film, Opt. Express 18 (2010) 11859–11866.
[20] B. Sutapun, M. Tabib-Azar, A. Kazemi, Pd-coated elastooptic fiber optic Bragg grating sensors for multiplexed hydrogen sensing, Sens. Actuators B: Chem. 60 (1999) 27–34.
[21] B. Michael, P.C. Kevin, B. Matrika, R.S. Philip, M. Mokhtar, Active fiber Bragg grating hydrogen sensors for all-temperature operation, IEEE Photonics Technol. Lett. 19 (2007) 255–257.
[22] K. Schroeder, W. Ecke, R. Willsch, Optical fiber Bragg grating hydrogen sensor based on evanescent-field interaction with palladium thin-film transducer, Opt. Lasers Eng. 47 (2009) 1018–1022.
[23] H.J. Patrick, A.D. Kersey, F. Bucholtz, Analysis of the response of long period fiber gratings to external index of refraction, J. Lightwave Technol. 16 (1998) 1606–1612.
[24] A. Cusano, P. Pilla, L. Contessa, A. Iadicicco, S. Campopiano, A. Cutolo, M. Giordano, G. Guerra, High-sensitivity optical chemosensor based on coated long-period gratings for sub-ppm chemical detection in water, Appl. Phys. Lett. 87 (2005) 234105.
[25] J. Zhang, X. Tang, J. Dong, T. Wei, H. Xiao, Zeolite thin film-coated long period fiber grating sensor for measuring trace organic vapors, Sens. Actuators B: Chem. 135 (2009) 420–425.
[26] J. Villatoro, M.P. Kreuzer, R. Jha, V.P. Minkovich, V. Finazzi, G. Badenes, V. Pruneri, Photonic crystal fiber interferometer for chemical vapor detection with high sensitivity, Opt. Express 17 (2009) 1447–1453.
[27] G. Gauglitz, A. Brecht, G. Kraus, W. Nahm, Chemical and biochemical sensors based on interferometry at thin (multi-)layers, Sens. Actuators B: Chem. 11 (1993) 21–27.
[28] D. Reichl, R. Krage, C. Krumme, G. Gauglitz, Sensing of volatile organic compounds using a simplified reflectometric interference spectroscopy setup, Appl. Spectrosc. 54 (2000) 583–586.
[29] J. Zhang, M. Luo, H. Xiao, J. Dong, Interferometric study on the adsorption-dependent refractive index of silicalite thin films grown on optical fibers, Chem. Mater. 18 (2005) 4–6.
[30] J. Liu, Y. Sun, X. Fan, Highly versatile fiber-based optical Fabry–Pérot gas sensor, Opt. Express 17 (2009) 2731–2738.
[31] J. Liu, Y. Sun, D.J. Howard, G. Frye-Mason, A.K. Thompson, S.-J. Ja, S.-K. Wang, M. Bai, H. Taub, M. Almasri, X. Fan, Fabry–Pêĭrot cavity sensors for multipoint on-column micro gas chromatography detection, Anal. Chem. 82 (2010) 4370–4375.
[32] C. Martínez-Hipatl, S. Muñoz-Aguirre, G. Beltrán-Pérez, J. Castillo-Mixcóatl, J. Rivera-De la Rosa, Detection of volatile organic compounds by an interferometric sensor, Sens. Actuators B: Chem. 147 (2010) 37–42.
[33] A. Thangawng, R. Ruoff, M. Swartz, M. Glucksberg, An ultra-thin PDMS membrane as a bio/micro–nano interface: fabrication and characterization, Biomed. Microdevices 9 (2007) 587–595.

## Biographies

**Karthik Reddy** received his B.S. and M.S. in Electrical Engineering from Texas A&M University in 2006 and 2009, respectively. He is currently pursuing a Ph.D. in Electrical Engineering at the University of Michigan. His research interests include applications of nanotechnology in chemical vapor sensing and miniaturized gas chromatography systems.

**Yunbo Guo** received his B.S. in Mechanical Engineering and M.S. degree in Optical Engineering from Tsinghua University, China in 2002 and 2005, respectively and his Ph.D. in Electrical Engineering (specialized in Optics) and Nanobiology Certificate from the University of Michigan in 2010, where developed a label-free photonic crystal biosensor that is being commercialized. Currently he is a postdoctoral researcher in the Biomedical Engineering Department, working on a nanofluidic Fabry–Pérot biosensor with integrated flow-through nanohole arrays. His research interests include optical biological and chemical sensors, optofluidics, photonic crystal, ultrasound generation and detection, and nanophotonics.

**Jing Liu** received her B.S. and M.S. degrees in Optoelectronic Engineering Department from Huazhong University of Science and Technology, China. She is currently pursuing a Ph.D. in Biomedical Engineering Department at University of Michigan. Her research interests include developing optical based vapor sensor and miniaturized gas chromatography system.

**Wonsuk Lee** received his B.S. and M.S. in Electrical Engineering from the Seoul National University in 2006 and 2009, respectively. He is currently a pursuing his Ph.D. in Electrical Engineering at the University of Michigan. His research interest includes optofluidic lasers based on ring resonators.

**Maung Kyaw Khaing Oo** received his B.S. from Yangon University, M.S. from National University of Singapore and Ph.D. from Stevens Institute of Technology in 2010. He is currently a postdoctoral research fellow at Biomedical Engineering Department, University of Michigan. His research interests include nanotechnology based ultra-trace detection and drug delivery. He is a member of ASME, OSA, and SPIE.

**Xudong Fan** received his B.S. and M.S. from Peking University in 1991 and 1994, respectively, and Ph.D. in physics and optics from Oregon Center for Optics at the University of Oregon in 2001. Between late 2000 and 2004, he was a project leader at 3 Company on fiber optics and photonic sensing devices for biomedical applications. In August of 2004, he joined the Department of Biological Engineering at the University of Missouri as an assistant professor. In January of 2010, he joined the Biomedical Engineering Department at the University of Michigan as an associate professor. Prof. Fan's research includes photonic bio/chemical sensors, micro/nano-fluidics, and nano-photonics for disease diagnostics and bio/chemical molecular analysis. He has over 60 peer-reviewed publications and over 10 issued/pending patents. He is a recipient of 3M Non-Tenured Faculty Award (2004, 2005, and 2006), American Chemical Society Petroleum Research Junior Faculty Award, the Wallace H. Coulter Early Career Award (Phase I and Phase II), and the National Science Foundation CAREER Award.